

Starting Analysis of Squirrel Cage Induction Motors 1000 kW by Variable Frequency Drive in Power System, Case study: Tabriz Pump station

1st Farhad Muhsin Mahmood¹, 2nd Mahdi Rahnamaei Hashjin²
farhad.mahmood@uoh.edu.iq¹, mahdi.rahnamaei@shahrood.ac.ir²

1. Department of Physics, College of Science, University of Halabja, Halabja, Iraq.

2. Faculty of Electrical Engineering, Shahrood University of Technology, Semnan, Iran.

Corresponding author: Mahdi Rahnamaei Hashjin, mahdi.rahnamaei@shahrood.ac.ir

Co-authors: Farhad Muhsin Mahmood: farhad.mahmood@uoh.edu.iq

Received: 21-09-2022, **Accepted:** 02-11-2022, **Published online:** 23-12-2022

Abstract. In petroleum industrial systems, analysis of power systems should be considered to exploit system reliability and prevent change in process performance during starting in equipment such as induction motors and industrial pumps. Medium-voltage induction motors are essential electrical machines in the oil, petrochemical, and process industries; therefore, the study of induction motors is an integral part of the analysis of power system. The starting current of induction motors is 5 to 7 times greater than the nominal current at the moment of starting until it reaches the nominal torque. This starting current will result in the motors and transformer and voltage drop in users' appliances connected to the electric grid to the extent that it might even cause a shutdown in the grid or not start the motor. In this paper, the starting of squirrel cage induction motors 1000kW by variable frequency drive in Tabriz pump station has been analysed by the ETAP 19.0.1 software.

Keywords: starting induction motors, squirrel cage induction motor, ETAP, starting current, petroleum industrial.

Introduction

In most oil, gas, and petrochemical industries, medium-voltage induction motors are needed for providing power to stimulate machines such as pumps and compressors. The advantages of these motors can be referred to as high reliability, low maintenance cost, and the possibility of starting the motor under load, which increase the use of these motors in process industries. Hence, induction motors start on the voltage of 6 and 11 kV. In a medium-voltage power grid, while starting an induction motor in an industrialized zone, the motor operates as a small impedance in the power grid; therefore, due to the low impedance of the motor in the grid, the starting current increases dramatically; in this situation, the current will be 5 to 7 times greater than the primary nominal current of the motor; this will cause an intense

increase in the bus current, as well as an intense voltage drop in nearby voltage consumers. This voltage drop will be significant in the low-voltage grids (0.42 kV) and lighting loads. Moreover, since the motor's starting torque is also dependent on the motor's terminal voltage, if the voltage drop is over 15 %, the motor may not be started to reach its nominal speed. The most effective way of electrical submersible pumps regulation is to use a variable frequency drive. At the same time, the reliability of a high-voltage multilevel frequency converter without reserve power cells exceeds insignificantly by no more than 5% for any operating time. The use of a high-voltage multilevel frequency converter with one reserve power cell in each phase provides an increase in reliability of up to 15...20% with up to 200,000 hours of operation. A further increase in the number of power cells does not give such a significant increase in reliability [1]. The control strategy for the overall system is developed and verified in the

MATLAB/SIMULINK platform. The results show that the proposed converter-fed induction motor drive performs satisfactorily at all operating frequencies [2]. Also, in another research, the capacitor bank has been used to increase the power factor and minimize the grid's voltage drop [3]. This paper presents a simple converter for driving three-phase induction motor from three-phase AC supply by using the variable frequency drive in feedback. Hence, the speed of induction motor is controlled by variable frequency device automatically through controller. It is simple and efficient method to control the speed because speed depends upon voltage, pole and frequency. Poles are fix inbuilt in the motor therefore we cannot change it and speed control through VFD is simple and energy efficiency method [4]. An article analysed the starting of electric motors in the power grid [5]. V. Kolev, and I. Zlateva reported that the introduction of VFD for driving mechanisms of high-power consumption (pumps and fans) in power plants may result in decrease towards the motor internal consumption which is between 2 – 3% [6]. In another research, the starting of medium-voltage induction motors is carried out in an industrialized zone; this study analysed static and dynamic starting [7]. Generally, Variable Frequency Drives (VFDs) allow to operate motors and pumps at the precise speed needed for the process and energy saving. Therefore, the Nuclear Power Plant (NPP) model was developed using Electrical Transient Analysis Program (ETAP) software and was benchmarked for Advanced Power Reactor 1400 MW electricity (APR1400). The analysis was performed with VFD installed and without VFD. The new approach for Condensate Pump (CP) energy saving calculation using VFD was introduced, and the results were confirmed by the ETAP model simulation results [8]. To minimize voltage disturbances and maintain quality of the power supply to customers, the paper presents clear limits for maximum allowable motors' starting currents and corresponding maximum electrical power ratings. The shared 11kV is a ring designed to feed more than one customer. The criterion, in this case, is to start two customers' motors at two different rings at the same time and observe the rapid voltage change at other customers fed from the same rings [9]. Capacitors have been used as drivers to increase the reduced voltage in the system at the starting moment and increase the reactive power generation [10]. A new Modular Double-Cascade multilevel converter topology with a six-winding isolation transformer

were presented. Owing to the modularity, the proposed topology is a flexible solution in motor and generator applications. The Total Harmonic Distortion of the output voltage is low compared with two-level converters because of the multiple series-connected power modules. The symmetric magnetic coupling between sub modules ensures inherent energy sharing and DC-link voltage balancing. The application fields of the proposed converter are diverse, including general medium-voltage motor and generator applications. Further, an interconnection of grids and voltage transformation are possible with the modular double-cascade converter topology [11]. Presented in [12] a new starting system for three-phase induction motors has been considered. The proposed starting system uses a part-winding and capacitors to start up, run and improve the power factor. A two-dimensional finite element magneto dynamic model of a three-phase induction motor has been used to analyse the proposed motor configuration. Several steady-state and time stepping simulations has been done, and they demonstrate the proposed motor has a starting line current of 60% of the conventional motor starting current and starting torque about 50% of the conventional motor starting torque. It is also demonstrated the full-load efficiency of the proposed motor is the same as the conventional motor full load operation and the power factor of the proposed motor is near to the unity [12]. During a first general start up using star-delta switches in all motors, the 1.85 MW, 3.3 kV Fan Motor of the Cement Mill section has presented an unacceptable voltage drop. Using a soft starter for this motor has reduced its voltage sag within the permissible limits and a smooth start up is accomplished. The highest voltage sag recorded is approximately 7%, at the 710 kW, 0.69 kV, and Filter Fan Motor of the Coal Mill section [13]. When a shunt active filter is put in service to take care of the harmonic and reactive power requirements of the controller and induction motor, it is found that the main current decreases drastically, with the THD level falling within 5%. In all, it can be stated that a shunt active filter can be very useful to reduce the current amplitude and pollution level substantially when an AC voltage controller fed induction motor drive is employed in certain applications like fans or centrifugal pumps. This will be a very useful scheme especially in industries where 6 multiple induction motors of large capacity are frequently started from a 3-phase supply using soft-start [14]. Hence, in this

paper, the starting of the induction motor of 1000 kV at the Tabriz pump station and different modes for operating of the squirrel cage induction motors will be discussed in the 6 kV grid. For the purpose of reducing of the starting current, the variable frequency drive method will be analysed by the ETAP 19.0.1 software.

1. Starting Analysis of Induction Motors

Squirrel cage induction motors are theoretically a self-starter; the stator of these motors, which is made by windings, creates a rotating magnetic field by connecting to a three-phased voltage source; this will create an induced magnetic field in the rotor's conductors. According to Faraday's and Lenz's laws, the stator's and rotor's magnetic fields interact with one another, causing rotation and torque in the motor [15]. At the starting moment, induction motors are stationary and such as short-circuited transformers. When the voltage is applied to the stator, a large current, named "Locked rotor current," will pass through the rotor. LRC current is a function of the motor's terminal voltage and design parameters. This current is about 5 to 7 times greater than the motor's initial current, which results in a voltage drop in the system alongside disruptions for the nearby voltage consumers and loads in the power system. The value of this voltage drop depends on the starting impedance and power system [16]. Due to the structure of the induction motor, in static mode, the starting power coefficient is low and about 10 to 20 percent. The rotor's impedance Z_2 is obtained by Equation (1):

$$Z_2 = \sqrt{R_2^2 + X_2^2} \quad (1)$$

Where X_2 is the rotor reactance and R_2 is the rotor resistance per phase; thus, the starting power factor will be:

$$\cos \varphi = \frac{R_2}{\sqrt{R_2^2 + SX_2^2}} \quad (2)$$

The torque-speed curve of the induction motor has been plotted in figure 1. At the starting moment, a current about 6.8 times greater than the starting current will pass through the motor. As the motor torque increases, the starting current decreases, and when the motor's speed reaches

80 percent of the nominal speed, the current drops significantly [17].

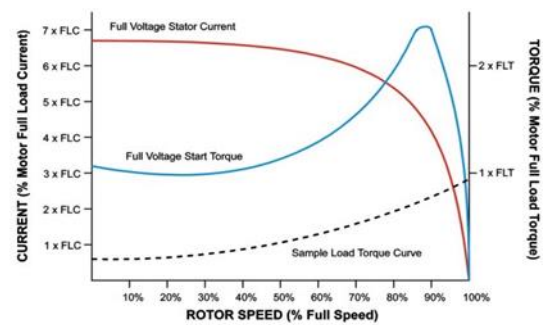


Fig. 1. Torque-speed curve of the induction motor

A high starting current can affect the insulation of the winding in induction motors and may damage the motor insulation by increasing the motor's internal temperature. Therefore, to control the starting current of induction motors, different methods are used to prevent high starting current [18]:

- Autotransformer starter: In this method, the input voltage is controlled by an autotransformer. At first, the reduced input voltage is given to the motor, and then the voltage increases until it reaches the nominal value. (Nominal load)
- Star-delta starter: During the motor starting, in order to reduce the starting current, the motor is operated star connection. As the motor speed increases to reach the nominal value and the fluctuations reduce, the motor windings are changed into delta connection. The starting current is calculated as:

$$v_p = \frac{V_L}{\sqrt{3}} \quad (3)$$

$$I_p = \frac{v_p}{Z} = \frac{V_L}{\sqrt{3} \times Z} = I_{LY} \quad (4)$$

$$I_{LY} = \frac{1}{3} I_{L\Delta} \quad (5)$$

Where V_L is line voltage, V_p is phase voltage, I_p is phase current, I_{LY} is line current (star), and $I_{L\Delta}$ is line current (delta).

- Double squirrel cage motor: In this method, with the aim of controlling the starting current, the motor is designed as a double squirrel cage. In this design, the motor consists of two cages; the outer cage must generate torque for starting the motor, and the inner cage has to generate torque at the steady-state model of

the motor. The rotor's frequency is calculated from Eq. (6):

$$f_r = Sf \quad (6)$$

Where f_r is rotor's frequency, S is motor's fluctuations, and f is the power system frequency.

- Current control by resistance: In this method, the rotor's current will be controlled by a resistance in the rotor's circuit. The current value is inversely proportional to the impedance; thus, the current will decrease as the resistance value increases. If E is equal to the inductive voltage in the rotor, R and X are, respectively, rotor's resistance and rotor's reactance; according to Equation (7), the rotor's current formula is:

$$I_2 = \frac{E_2^2}{\sqrt{R_2^2 + SX_2^2}} \quad (7)$$

Consequently, the starting torque is calculated by Eq. (8):

$$T_{st} = K_2 \frac{R_2}{R_2^2 + X_2^2} \quad (8)$$

$$K_2 = \frac{3P}{\omega_s} E_2^2 \quad (9)$$

Where, T_{st} is the starting torque, K is rotor factor, ω_s is rotor's rotational speed, and P is the number of poles in the motor.

- Variable frequency drive: Controlling the motor's starting current via variable frequency drive is one of the methods for operating high power induction motors. In order to linearly control the motor's speed, these drives apply a frequency that is less than the nominal frequency to the motor at the starting moment [8].

2. Modelling of Power Grid of Tabriz Case study (Tabriz pump station)

To study and analyse the starting of squirrel cage induction motors at the Tabriz pump station, the Tabriz power grid model with neighbouring pump stations for load flow study, along with short circuit and starting motor analysis have been considered. Given that the adjacent stations have process activity (with oil) going on, it is necessary to analyse the impacts of starting this motor on

their voltage profile; because it might cause a severe problem in their performance due to the voltage drop at the adjacent stations. Therefore, for the verification purposes, modelling has been done from the 132 kV power grid to the Tabriz pump station in ETAP 19.0.1 software. Based on [19], the short circuit power of the 132 kV power grid has been considered as 10000 MVA. The existing power grid has three oil pump stations. Figure 2 illustrates a single line diagram of the Tabriz power Grid.

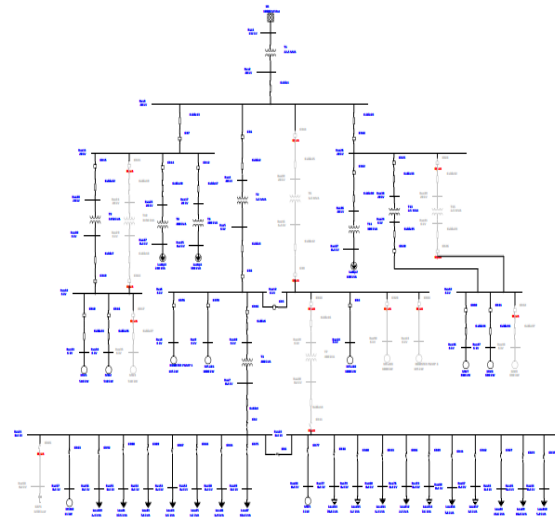


Fig. 2. Single Line Diagram of Tabriz Power Grid

Fig. 3 shows Tabriz pump station, which has three squirrel cage induction motors with a power of 1000 kW, these are fed by two 3.5 MVA parallel transformers. One of the transformers is available and another is on standby.

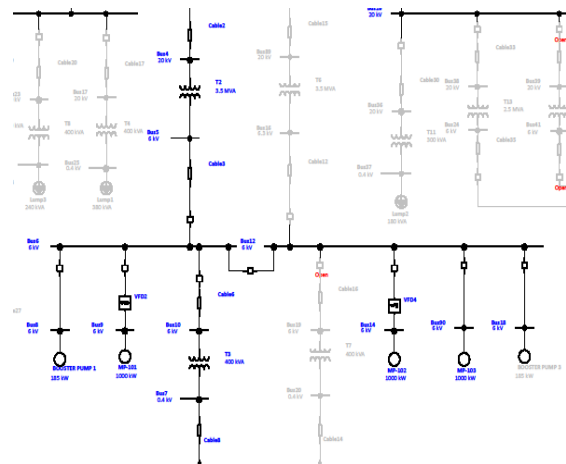


Fig. 3. Single Line Diagram of Tabriz Pump Station

Transformers details have been reported in the table below:

Table 1. Transformer Parameters

| Tag | Rating | | | %Z | X/R |
|-------|--------|----------|---------|------|-----|
| | MVA | Prim. kV | Sec. kV | | |
| T_2 | 3.5 | 20 | 6 | 7.05 | 8.5 |
| T_6 | 3.5 | 20 | 6 | 7.05 | 8.5 |

There are two motors in the service mode and one motor in the standby mode in this arrangement. If one of the motors fails to operate or gets out of the circuit, that motor will be removed from the circuit, and the motor on standby mode comes into service; this way, no problems occur during the process. Based on Fig. 2, the motors are fed by bus bar 6. The characteristics of induction motors are as follows:

Table 2. Three-phase Induction Motors Data (MP101, MP102, MP103)

| | | |
|----------------------|-----------|------|
| Nominal Voltage (kV) | 6 | |
| Nominal Current (A) | 113 | |
| Power (kW) | 1000 | |
| Frequency (Hz) | 50 | |
| Power Coefficient | 100% load | 0.9 |
| | 75% load | 0.87 |
| | 50% load | 0.85 |
| Efficiency | 100% load | 97 |
| | 75% load | 95.5 |
| | 50% load | 94.8 |
| X_s (Ω) | 11.13 | |
| R_s (Ω) | 1.78 | |
| X_r (Ω) | 11.01 | |
| R_r (Ω) | 1.58 | |
| X_m (Ω) | 346.6 | |
| %S | 0.6 | |
| %LRC | 550 | |
| $\cos\phi_r$ | 14.2 | |

Fig. 4 shows the internal schematic of an induction motor. R_s Which is stator's resistance, X_s is stator's reactance, R_r is rotor's resistance, X_r is rotor's reactance, and motor's inducted reactance has been demonstrated in this figure.

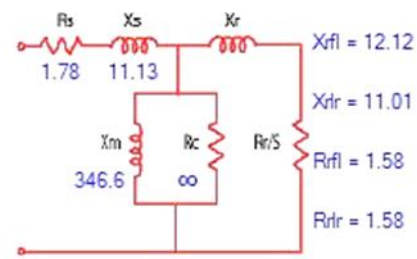


Fig. 4. Internal Schematic of a 1000 kW Induction Motor

3. Analysis of Tabriz pump station

3.1. Load Flow Study

The load flow study of the power grid has been done by Newton-Raphson method. According to that in busbar Number 6, two 1000 kW motors have been started, no voltage drops, and overload are observed in the station. The voltage drop is 0.069 and the power factor of the motor is 0.9. In the load flow study, all loads of Tabriz pump station are powered by 3.5 MVA transformer.

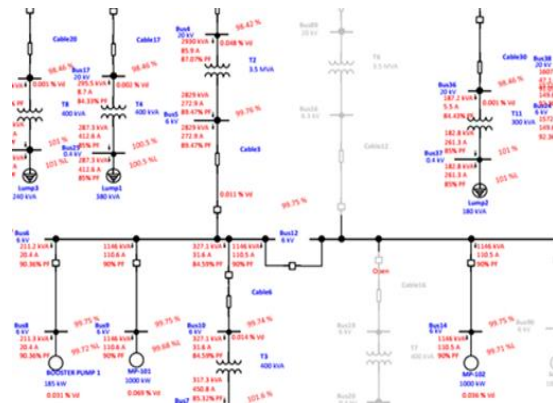


Fig. 5. Single line diagram of Tabriz pump station, load flow study (Newton-Raphson method)

Table 3. Transformer and Induction Motor Parameters (nominal voltage, current, power factor, voltage drop)

| TAG | Voltage % | Current A | $\cos\phi$ % | V_d % |
|---------------|-----------|-----------|--------------|---------|
| MP-101 | 99.75 | 110.6 | 90 | 0.069 |
| MP-102 | 99.75 | 110.6 | 90 | 0.069 |
| T2 3.5 MVA | 99.76 | 272.8 | 89.46 | 0.011 |
| T3 400 VA | 99.74 | 450.8 | 85.32 | 0.115 |

According to Table 3, the voltage drop during continuous operation of induction motors at the station is less than 2% and is acceptable. The voltage at the T2 transformer terminal has dropped by 0.24%, which is due to the presence of two 1000 kW motors and an active pump booster at the station. The low voltage loads of the station are supplied by transformer T6. In this transformer, the voltage drop is acceptable and there will be no problem with the connected loads (Voltage drop less than 2%).

3.2. Short Circuit Study

To calculate the short circuit current in the Tabriz pump station in ETAP software, calculations have been performed based on IEC 60909 standard. Figure 6 shows a single line diagram of the Tabriz pump station during the short three-phase to ground, according to [20].

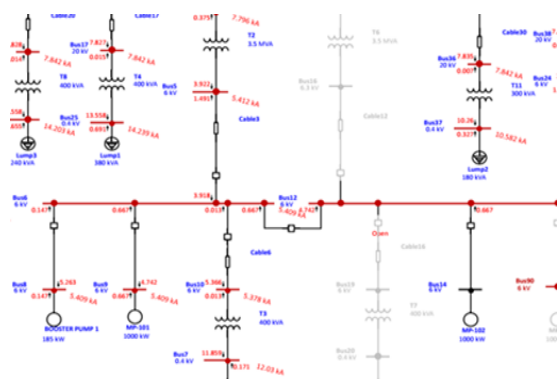


Fig. 6. Single line diagram of Tabriz pump station, three-phase short circuit to ground

The parameters of the short circuit of the power grid of Tabriz are specified in Table 4.

Table 4. Short-Circuit Current Values of Transformers, Busbar, and Induction Motors

| TAG | SHORT CIRCUIT Current kA | |
|---------|-----------------------------|-------|
| MP-102 | 5.409 | |
| MP-102 | | |
| MP-103 | | |
| BUS 6 | 5.409 | |
| T2 | HV | 7.796 |
| 3.5 MVA | MV | 5.412 |
| T3 | MV | 5.378 |
| 400 kVA | LV | 12.03 |

When a short circuit occurs, the magnitude of short circuit current in the Tabriz pump station is 5.4 kA. The maximum short circuit current of the Tabriz pump station is equal to the largest load consumption, which is a 1000 kW motor. If a parallel transformer is also operated at the station, the amount of short circuit current will increase to 8.17 kA. The largest short circuit level for a low-voltage transformer is 12.03 kA.

3.3. Static Motor Analysis

In this section, three methods of starting a motor are presented. Because the voltage drop at the starting moment should not be more than 15% [21] and to prevent problems for the station's performance; the following methods are considered to be the most appropriate starting methods:

3.3.1. First Case Study: One transformer in service and one of the motors for starting:

Fig. 7 shows the single-line diagram of the first case study. In this case, a transformer with a power of 3.5 MVA feeds Tabriz pump station, and a 1000 kW motor is started. According to the table 5 the following data were obtained:

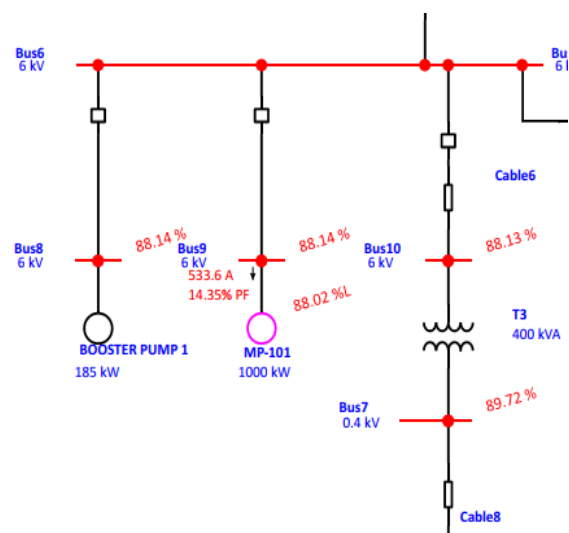


Fig. 7. Single line diagram of the first case study for starting an induction motor (One transformer + one motor)

Table 5. Busbar and induction motor parameters at first case study (nominal voltage, current, power factor)

| | Voltage % | Current A | $\text{Cos}\phi$ % |
|--------|-----------|-----------|--------------------|
| MP-101 | 88.02 | 533.6 | 14.35 |
| Bus 6 | 86.41 | - | - |

Given the values of the table, in this case, the motor terminal voltage is less than 15 % at the starting moment, and the grid will reach stability after starting moment.

3.3.2. Second Case Study: One transformer in service and two motors for starting:

Fig. 8 shows the single line diagram of the second case study. In this case, a transformer with a power of 3.5 MVA feeds the Tabriz pump station, and two 1000 kW motors are started. According to table 6, the following data were obtained:

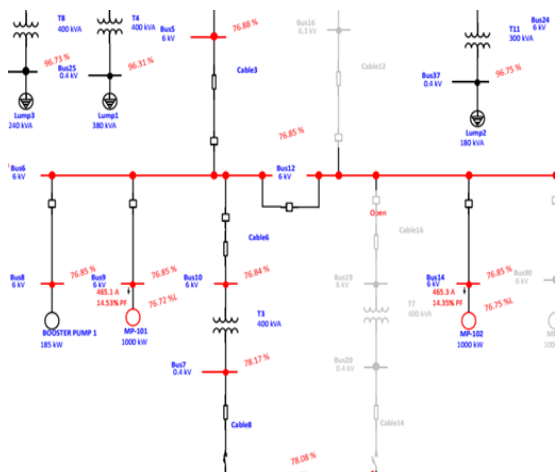


Fig. 8. Single line diagram of the second case for starting an induction motor (One transformer + two motor)

Table 6. Busbar and induction motor parameters at second case study (nominal voltage, current, power factor)

| | Voltage % | Current A | $\text{Cos}\phi$ % |
|--------|-----------|-----------|--------------------|
| MP-101 | 76.85 | 465.3 | 14.35 |
| MP-102 | 76.85 | 465.3 | 14.35 |
| Bus 6 | 76.85 | - | - |

Given the table values, in this case, the motor's terminal voltage is more than 15 % at the starting

moment; thus, the motor will not be started. Also, because of the high voltage drop in this station, low-voltage consumers will face shut down. Regarding the station's performance, this case is the worst case of starting the motor.

3.3.3. Third Case Study: one transformer and one motor available - one motor to starting:

Figure 9 shows a single line diagram of third case study. In this case, one motor is in service, and one motor is started. According to Table 7, the following data are obtained:

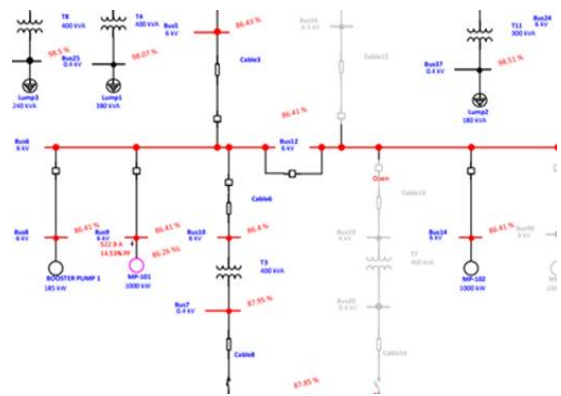


Fig. 9. Single line diagram of starting the third case study (one transformer and one motor available - one motor to starting)

Table 7. Busbar and induction motors parameter at third case study (nominal voltage, current, power factor)

| | Voltage % | Current A | $\text{Cos}\phi$ % |
|--------|-----------|-----------|--------------------|
| MP-101 | 86.4 | 523.1 | 14.35 |
| MP-102 | 86.4 | - | - |
| Bus 6 | 86.41 | - | - |

According to the values of the table 7, it is clear that, in this case, the motor terminal voltage is less than 15% and there is no problem at the moment of starting. Also, in low voltage distribution transformers, the voltage is acceptable, and blackouts and interruptions will not occur. This arrangement is the best possible method of starting; because when the first motor is running, the second motor is started, and the voltage drop is acceptable, and it follows the standard [21]. If one of the motors fails, the third motor (standby)

can replace the broken motor so that the operation of the pump station is not disturbed.

4. Dynamic motor analysis

4.1. Variable Frequency Drive Study:

Variable frequency drive consists of electronic power equipment to change input voltage and frequency to variable voltage and frequency at the output for a soft start in high power induction motors and industrial pumps. In VFD design, the voltage and output frequency are controlled by switching the thyristors. According to the equation (10), the voltage to frequency ratio is calculated for optimal VFD design. On this basis, the voltage to frequency ratio for the 6 kV power grid is as follows [10]:

$$\frac{V}{F} = \frac{6kV}{50} = 120\% \quad (10)$$

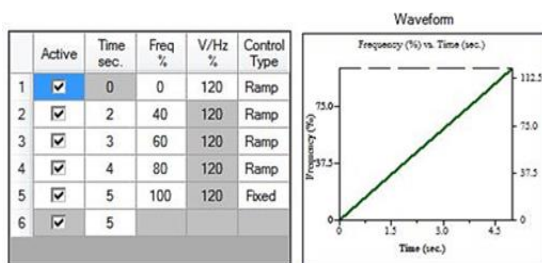


Fig. 10. Frequency-time curve, Variable frequency drive parameters (frequency steps)

Figure 10 shows the VFD linear curve. To control the motor speed up to the point it reaches to the nominal speed, five frequency steps have been considered. In the first step, the frequency value is 0 Hz, in the second step 40% (20 Hz), in the third step 60% (30 Hz), in the fourth step 80% (40 Hz), and in the fifth step with 100% frequency (50 Hz) the motor is started. As shown in Figure 11, when the motor is started by a variable frequency drive, after the moment of starting, the slip reaches its minimum value due to the increase of the motor speed and torque up to the maximum value. Figure 12 shows a curve of speed- time. The variable frequency drive is designed so that the motor speed increases linearly and will cause the motor to soft-start.

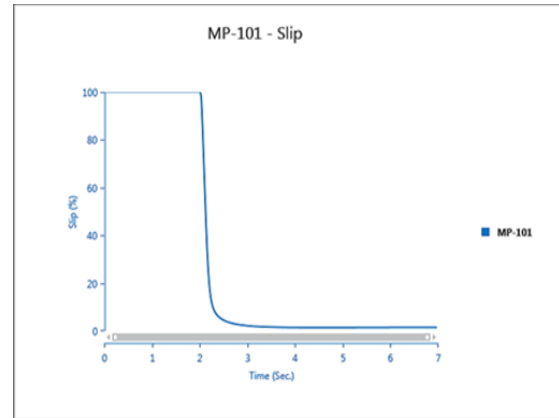


Fig. 11. Slip-time curve for Mp-101

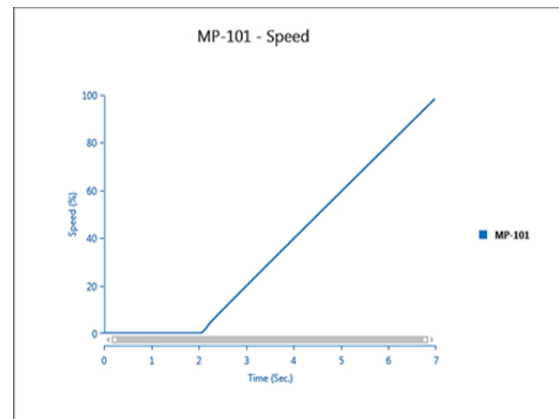


Fig. 12. Speed-time curve for Mp-101

Figure 13 shows the current-time curve of the motor in starting mode with a variable frequency drive. When the motor is started by the VFD, the initial current will be 65% of the rated current of the motor. In this case, without starting by VFD, the starting current will be 5 to 7 times the rated current of the motor. At the starting moment of the motor, 65% of the rated current will be used to generate the starting torque. Then, the torque increases exponentially to the nominal value. Figure 14 shows the motor starting torque-time curve.

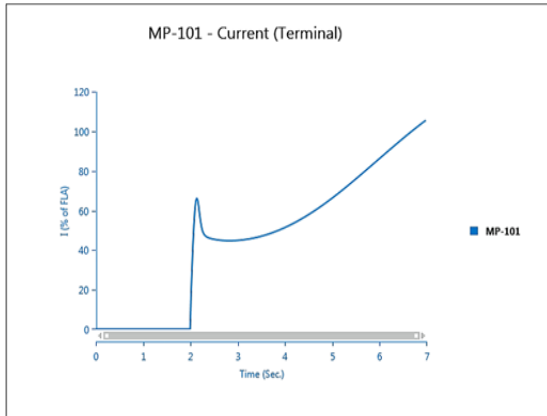


Fig. 13. Current-time curve for Mp-101

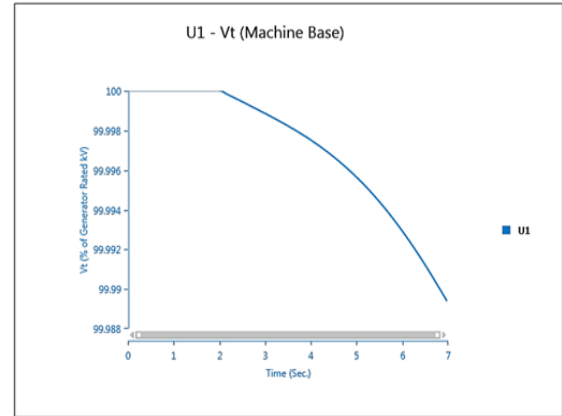


Fig. 16. Voltage-time curve 132 kV power grid

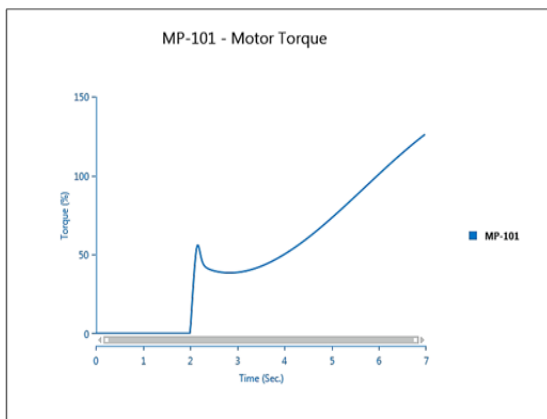


Fig. 14. Torque-time curve for Mp-101

Figures 15 and 16 show the voltage curves in the 132kV and 20kV power grid of Tabriz. At the moment of starting the motor by VFD, the 132 kV power grid, voltage drops by 2%. Also, in the 20kV grid, the voltage has decreased by 1.7%. These values are acceptable in the examined power grid.

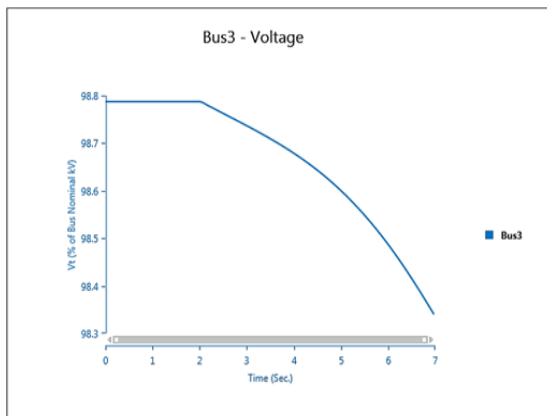


Fig. 15. Voltage-time curve 20 kV power grid

Conclusion

In this paper, in order to start the Tabriz pump station with squirrel cage induction motors, the Tabriz power grid was studied. Because the high starting current is caused by low impedance in the grid, nearby loads will face a significant voltage drop. Thus, the starting of motors in the power grid will affect the power quality and reliability of the system. For this reason, the direct starting of the motors was analysed in all cases. When two motors were fed from the grid simultaneously, the voltage drop in the motor's terminal exceeded the desired value; thus, to control the starting voltage and current, the motors were started by a variable frequency drive. According to the results and characteristic plots, it was demonstrated that by connecting motors to a variable frequency drive, two motors could be started simultaneously without causing a voltage drop in the station. Given that there are adjacent voltage consumers in the Tabriz power grid, there will be no change in voltage profile at the VFD starting case; in this case, the voltage, frequency, and starting current are controlled, and the grid is stable, in addition to the high reliability of the power grid, the maintenance cost also decreases considerably in this case.

References

- [1] I. Shafikov, M. Khakimyanov. (2020) 'Assessment of Reliability of the Electric Submersible Pump Variable Frequency Drive. 2020 International Conference on Industrial Engineering, Applications and Manufacturing (ICIEAM), 09 June 2020, Sochi, Russia.

- [2] S. Chakraborty, S. Maiti, A. Bharadwaj.Ch. (2020) A Novel AC/AC Modular Multilevel Converter for Medium Voltage Variable Frequency Vector Controlled Induction Motor Drives. 2020 IEEE International Conference on Power Electronics, Smart Grid and Renewable Energy (PESGRE2020).
- [3] Mutmainnah, Muhammad Fadli Azis and Julianti Habibuddin. (2020) Power factor correction of the industrial electrical system during large induction motor starting using ETAP power station. IOP Conf. Series: Materials Science and Engineering 885 (2020) 012009, doi:10.1088/1757-899X/885/1/012009.
- [4] M.A. Niazi, Q. Hayat, B. Khan, M.Afaq. (2020) Speed Control of Three-Phase Induction Motor using Variable Frequency Drive Control System. International Journal of Current Engineering and Technology, Vol.10, No.1.
- [5] Nikolay Matanov. (2019) Study of the impact of induction motors starting on the supply voltage. XVI-the International Conference on Electrical Machines, Drives and Power Systems ELMA 2019, 6-8 June 2019, Varna, Bulgaria, <https://doi.org/10.1109/ELMA.2019.8771585>.
- [6] V. Kolev, I.Zlateva. (2019) Application of variable frequency drives (VFD) with large 6 kV asynchronous motors. XVI-the International Conference on Electrical Machines, Drives and Power Systems ELMA 2019, 6-8 June 2019, Varna, Bulgaria.
- [7] Ashokkumar Parmar. (2018) Motor Starting Analysis of Industrial Plant. International Journal of Advance Engineering and Research Development (IJAERD) Volume 5, Issue 03, March-2018, e-ISSN: 2348 - 4470, print-ISSN: 2348-6406.
- [8] E.Zakaria Barie, C. Chang. (2018) Application of variable frequency drive on the condensate pump motors of APR1400 nuclear power plants for energy savings. JOURNAL OF INTERNATIONAL COUNCIL ON ELECTRICAL ENGINEERING 2018, VOL. 8, NO. 1, 179-189.
- [9] M. Ashaar, M. Jaber, H. Adel. (2018) Define the Limits of 11kV Motors Starting Current in Distribution Network. 2018 IEEE PES Asia-Pacific Power and Energy Engineering Conference (APPEEC), 10 December 2018, Kota Kinabalu, Malaysia.
- [10] Osita Oputa, Patrick I. Obi,Ifeanyichwukwu K. Onwuka. (2017) Induction Motor Starting Analysis and Start Aided Device Comparison Using ETAP. EJERS, European Journal of Engineering Research and Science Vol. 2, No. 7, July 2017 DOI: <http://dx.doi.org/10.24018/ejers.2017.2.7.348>.
- [11] A. Sankala, J. Korhonen1, J. Ström, J. Luukko1, P. Silventoinen, R. Komulainen, H. Sarén, N. Södö, D. Isaksson. (2015) IET Power Electron. 2015, Vol. 8, Iss. 9, pp. 1661-1669.
- [12] A. Gonzalez, M. A. Arjona. (2014) new starting system for three-phase induction motors by using a part-winding and capacitors. 7th IET International Conference on Power Electronics, Machines and Drives (PEMD 2014), 8-10 April 2014, Manchester, UK.
- [13] Evangelia K. Gkogkou, Chryso V. Daniel, Maria G. Gkeka, Efthymios Efthymiou, Christos G. Kaloudas,Grigoris K. Papagiannis. (2010) Short-Circuit Current Calculation and Motor Starting Analysis in a Cement Industry in Cyprus. 7th Mediterranean Conference and Exhibition on Power Generation, Transmission, Distribution and Energy Conversion 7-10 November 2010, Agia Napa, Cyprus (Paper No. MED10/196).
- [14] G.Bhuvaneswari, Charles S, Manjula G.Nair. (2008) Power Quality Studies on a Soft-Start for an Induction Motor. 2008 IEEE/PES Transmission and Distribution Conference and Exposition, 12 May 2008, Chicago, IL, USA.
- [15] Aung Zaw Latt. (2019) Three-Phase Induction Motor Starting Analysis Using ETAP. International Journal of Latest Technology in Engineering, Management & Applied Science (IJLTEMAS), Volume VIII, Issue IV, April 2019 | ISSN 2278-2540.
- [16] Piyush S. Patil, K. B. Porate. (2009) Starting Analysis of Induction Motor a Computer Simulation by ETAP Power Station. 2009 Second International Conference on Emerging Trends in Engineering & Technology. DOI: 10.1109/ICETET.2009.211.
- [17] Paul B. Steciuk, Greg Bow, Dwaraka S. Padimiti, Frederick D. Painter II. (2019) Practical Application of TRANSIENT-FREE Capacitor Switch (TFCS) Technology for Starting Large Induction Motors at a Texas Natural Gas Processing Plant. 2019 IEEE Petroleum and Chemical Industry Committee Conference (PCIC), DOI: 10.1109/PCIC30934.2019.9074495.
- [18] M. Habyarimana, D. G. Dorrell. (2017) Methods to Reduce the Starting Current of an Induction Motor. IEEE International Conference on Power, Control, Signals and Instrumentation Engineering (ICPCSI-2017), DOI: 10.1109/ICPCSI.2017.8392319.
- [19] IEC 60076-5 Power transformers-Specification - Part 5: Ability to withstand short circuit, Third edition 2006-02.
- [20] IEC 60909-0 Short-Circuit Currents in Three-phase a.c. Systems -Part 0: Calculation of Currents (including 2002 corrigendum 1) for systems up to 500k.
- [21] S. Kucuk, A. Ajder. (2022) 'Analytical voltage drop calculations during direct on line motor starting: Solutions for industrial plants. Ain Shams Engineering Journal,Volume 13, Issue 4, June 2022, 101.